

## ARTICLE OPEN



# Structural covariance of the ventral visual stream predicts posttraumatic intrusion and nightmare symptoms: a multivariate data fusion analysis

Nathaniel G. Harnett<sup>1,2</sup>, Katherine E. Finegold<sup>1</sup>, Lauren A. M. Lebois<sup>1,2</sup>, Sanne J. H. van Rooij<sup>3</sup>, Timothy D. Ely<sup>3</sup>, Vishnu P. Murty<sup>4</sup>, Tanja Jovanovic<sup>5</sup>, Steven E. Bruce<sup>6</sup>, Stacey L. House<sup>7</sup>, Francesca L. Beaudoin<sup>8</sup>, Xinming An<sup>9</sup>, Donglin Zeng<sup>10</sup>, Thomas C. Neylan<sup>11</sup>, Gari D. Clifford<sup>12,13</sup>, Sarah D. Linnstaedt<sup>9</sup>, Laura T. Germine<sup>12,14,15</sup>, Kenneth A. Bollen<sup>16</sup>, Scott L. Rauch<sup>2,14,17</sup>, John P. Haran<sup>18</sup>, Alan B. Storrow<sup>19</sup>, Christopher Lewandowski<sup>20</sup>, Paul I. Musey<sup>21</sup>, Phyllis L. Hendry<sup>22</sup>, Sophia Sheikh<sup>22</sup>, Christopher W. Jones<sup>23</sup>, Brittany E. Punches<sup>24,25</sup>, Michael C. Kurz<sup>26,27,28</sup>, Robert A. Swor<sup>29</sup>, Lauren A. Hudak<sup>30</sup>, Jose L. Pascual<sup>31,32</sup>, Mark J. Seamon<sup>32,33</sup>, Erica Harris<sup>34</sup>, Anna M. Chang<sup>35</sup>, Claire Pearson<sup>36</sup>, David A. Peak<sup>37</sup>, Robert M. Domeier<sup>38</sup>, Niels K. Rathlev<sup>39</sup>, Brian J. O'Neil<sup>40</sup>, Paulina Sergot<sup>41</sup>, Leon D. Sanchez<sup>42,43</sup>, Mark W. Miller<sup>44,45</sup>, Robert H. Pietrzak<sup>46,47</sup>, Jutta Joormann<sup>48</sup>, Deanna M. Barch<sup>49</sup>, Diego A. Pizzagalli<sup>1,2</sup>, John F. Sheridan<sup>50,51</sup>, Steven E. Harte<sup>52,53</sup>, James M. Elliott<sup>54,55,56</sup>, Ronald C. Kessler<sup>57</sup>, Karestan C. Koenen<sup>58</sup>, Samuel A. McLean<sup>59,60</sup>, Lisa D. Nickerson<sup>2,61</sup>, Kerry J. Ressler<sup>1,2</sup> and Jennifer S. Stevens<sup>3</sup>

© The Author(s) 2022

Visual components of trauma memories are often vividly re-experienced by survivors with deleterious consequences for normal function. Neuroimaging research on trauma has primarily focused on threat-processing circuitry as core to trauma-related dysfunction. Conversely, limited attention has been given to visual circuitry which may be particularly relevant to posttraumatic stress disorder (PTSD). Prior work suggests that the ventral visual stream is directly related to the cognitive and affective disturbances observed in PTSD and may be predictive of later symptom expression. The present study used multimodal magnetic resonance imaging data ( $n = 278$ ) collected two weeks after trauma exposure from the AURORA study, a longitudinal, multisite investigation of adverse posttraumatic neuropsychiatric sequelae. Indices of gray and white matter were combined using data fusion to identify a structural covariance network (SCN) of the ventral visual stream 2 weeks after trauma. Participant's loadings on the SCN were positively associated with both intrusion symptoms and intensity of nightmares. Further, SCN loadings moderated connectivity between a previously observed amygdala-hippocampal functional covariance network and the inferior temporal gyrus. Follow-up MRI data at 6 months showed an inverse relationship between SCN loadings and negative alterations in cognition in mood. Further, individuals who showed decreased strength of the SCN between 2 weeks and 6 months had generally higher PTSD symptom severity over time. The present findings highlight a role for structural integrity of the ventral visual stream in the development of PTSD. The ventral visual stream may be particularly important for the consolidation or retrieval of trauma memories and may contribute to efficient reactivation of visual components of the trauma memory, thereby exacerbating PTSD symptoms. Potentially chronic engagement of the network may lead to reduced structural integrity which becomes a risk factor for lasting PTSD symptoms.

*Translational Psychiatry* (2022)12:321; <https://doi.org/10.1038/s41398-022-02085-8>

## INTRODUCTION

Traumatic memories in posttraumatic stress disorder (PTSD) can spontaneously intrude into a victim's thoughts, contributing to re-experiencing of the event, or prompting hypervigilance to potential cues that signal danger [1]. Though often assumed to reflect alterations in core threat neurocircuitry, the process of encoding, recalling, and directing attention to visual information in PTSD may also rely on visual circuitry that has been generally understudied [2]. Vividness of imagined scenes in those with PTSD has long been known to be positively related to frequency of posttraumatic flashbacks and nightmares, underscoring the potential clinical relevance of visual

processing in the disorder [3]. Putatively aberrant neurobiology of visuo-affective circuitry may thus help to clarify PTSD-related behavioral changes such as threat vigilance, flashbacks, nightmares, and intrusive thoughts [4–8].

The ventral visual stream may be particularly important for PTSD given its role in object recognition and categorization, and its interconnections with canonical threat-related regions such as the amygdala for processing of threat-relevant stimuli [9–14]. Early visual cortex regions (V1 and V2), the posterior/anterior inferior temporal lobe, and superior temporal sulcus are thought to be canonical regions of the ventral visual stream with known projections to regions such as the amygdala, medial temporal

A full list of author affiliations appears at the end of the paper.

Received: 22 June 2022 Revised: 14 July 2022 Accepted: 20 July 2022

Published online: 08 August 2022

lobe, and striatum [15]. Sensory information is thought to move from primary visual cortices along the pathway towards more anterior components wherein more complex and higher-order features tend to be represented. The ventral visual stream has also previously been proposed to be critical for the development of the prefrontal cortex (PFC) and executive functions including attention regulation [16]. Both animal model and human neuroimaging research also demonstrate that stress exposure modulates activity in neural regions of visual processing [17, 18]. Extant literature therefore suggests visual circuitry may be involved in stress-modulated threat responses, but limited work in PTSD has directly investigated potential disorder-relevant circuitry variability.

Consideration of visual circuitry may further the development of functional and structural magnetic resonance imaging (MRI)-based neural signatures of PTSD susceptibility. Prior functional MRI (fMRI) studies suggest amygdala reactivity to threat and connectivity to the PFC either before or relatively early after trauma is associated with greater risk to developing later PTSD symptoms [19–22]. However, ventral visual areas also show increased reactivity to threat in chronic PTSD [23] and amygdala to visual cortex connectivity is related to later PTSD symptoms above and beyond current PTSD symptoms [22]. Moreover, structural MRI research suggests hippocampal volume and uncinate fasciculus microstructure are predictive of PTSD, though these findings are mixed [24–30]. Other white matter imaging research, however, has found that microstructure of visual association tracts such as the inferior fronto-occipital fasciculus and inferior longitudinal fasciculus in the early aftermath of trauma is related to PTSD development [31]. Thus while neurobiology of threat circuitry is important, integration of functional and structural correlates of visual circuitry may enhance our understanding of the neurobiology of PTSD susceptibility.

Multimodal data fusion approaches to brain imaging data may be better suited to uncovering affective visual neurocircuitry relevant to PTSD than previously used unimodal approaches. Multivariate analyses allow for simultaneous integration of information across multiple imaging modalities to identify associations with PTSD symptoms, thus increasing the overall power of MRI data to identify PTSD-susceptible phenotypes. Prior work observed multimodal patterns of fMRI and positron emission tomography (PET) activation distributed across threat neurocircuitry that also included thalamus, extrastriatal, and primary visual cortex differentially associated with PTSD and traumatic brain injury-related dysfunction [32]. Similarly, we have previously observed an association between the strength of a multimodal ventral visual stream structural covariance network and early PTSD symptoms after trauma in a distinct, smaller trauma cohort [33]. Together, the prior findings highlight the increased power and utility of multimodal neuroimaging for dissecting trauma-related disorder phenotypes and the potential role of both threat and visual neurocircuitry. Whether changes in structure of the ventral visual stream over time, or potential relationships to brain function, are related to PTSD symptoms remains unclear.

In the present study, we utilized data from the large, prospective, longitudinal Advancing Understanding of Recovery after Trauma (AURORA) study to investigate multimodal MRI markers of PTSD. We first investigated if a previously observed structural covariance network (SCN) of the ventral visual stream (VVS) would be replicated in a separate, multisite, and demographically heterogeneous dataset. We hypothesized that individual variability in the strength of the SCN would be positively related to acute PTSD symptoms. We also examined the relationship between variability in the SCN loadings and post-trauma nightmare symptoms as an index of vision-related posttraumatic disturbance. In addition, we investigated if the VVS SCN would be related to threat-related neural reactivity or connectivity patterns previously shown to be related to PTSD susceptibility in

emergency department cohorts. Finally, we evaluated if changes in SCN loadings were associated with changes in PTSD symptoms over time. The present findings provide a robust characterization of a multimodal structural covariance network of the ventral visual stream in recent trauma victims and establishes a new framework for potential affective-visual circuitry that may be critical to understanding PTSD susceptibility.

## METHODS

Data from the present analyses were obtained as part of the AURORA Study, a multisite longitudinal study of adverse posttraumatic neuropsychiatric sequelae. Details of the larger AURORA project are described in the parent and recent reports [22, 34–36]. Briefly, trauma-exposed participants were recruited from Emergency Departments (ED) from across the United States. Trauma was defined as a medical accident requiring admission to the ED, and participants who experienced events such as a motor vehicle collision, high fall (>10 feet), physical assault, sexual assault, or mass casualty incidents were automatically included in the study. Other trauma exposures were also qualifying if: (a) the individual responded to a screener question that they experienced the exposure as involving actual or threatened serious injury, sexual violence, or death, either by direct exposure, witnessing, or learning about the trauma and (b) the research assistant agreed that the exposure was a plausible qualifying event. Trauma was a necessary inclusion criterion for the present study, and no participants without trauma were included. Frequency of the broad class of trauma exposures endorsed by participants are included in Table S1. Data were initially intended to be collected from 439 participants recruited between 09/25/2017 and 07/31/2020. Of the recruited participants, no MRI data were collected from 53 participants. Further, the present multimodal data fusion analysis required participants to have completed both anatomical T1-weighted and diffusion weighted imaging (DWI). Thus, we excluded participants without either data type or whose data did not pass quality control procedures (described below). In total, 278 participants were included in the multimodal data fusion analyses. A subset of individuals ( $n = 83$ ) also had usable MRI data from a follow-up imaging session 6 months after trauma exposure. All participants gave written informed consent as approved by each study site's Institutional Review Board.

## Demographic and psychometric data collection

Initial participant demographic and psychometric data were collected after admission to the ED (Table 1). PTSD symptoms were assessed using the PTSD Checklist for DSM-5 (PCL-5) [37], a 20-item self-report questionnaire on symptom expression and severity. Participants' PTSD symptoms were assessed within the ED (i.e., past 30 days prior to trauma), 2 weeks, 8 weeks, 3 months, and 6 months after trauma exposure. For the present analyses, we focused on prior (30 days prior to ED), 2-week and 6-month PTSD symptoms post ED given our a priori interests and to limit the number of potential comparisons. The 2-week assessment queried participant symptoms in the past 14 days while the 6-month assessment queried participant symptoms in the past 30 days. Participants' depression symptoms were also assessed using the Patient-Reported Outcomes Measurement Information System (PROMIS) Depression instrument from the PROMIS short form 8b [38]. T-scores were derived from total responses to eight items scored on a Likert scale from 1 (never) to 5 (always). Participants' prior life trauma was assessed using the Life Events Checklist version 5 (LEC-5) [39]. The checklist assessed prior exposure to traumatic events such as natural disasters, accidents, assaults, etc. that (a) happened directly to the participant, (b) were witnessed by the participant, (c) the participant learned happened to someone close to them, or (d) the participant was exposed to details of it due to their occupation. Responses to all questions were summed to derive a prior trauma index and participants who did not respond to all questions were coded as missing. Participants' symptoms of nightmares were assessed two weeks after trauma using the Clinician Administered PTSD Scale IV [40, 41]. Specifically, participants were asked, in the past two weeks, (1) how often they had unpleasant dreams and (2) how much distress or discomfort did their unpleasant dreams cause? Participants scored each question on a scale from 0 to 4. Nightmare frequency was defined as participant responses to question one. Nightmare intensity was defined as participant responses to question two. Nightmare severity was defined as the sum of responses to questions one and two.

**Table 1.** Participant demographics.

| Characteristic  | Mean (SD) or n (%)        |
|---|---------------------------|
| Age   | 33.99 (12.83)             |
| Sex assigned at birth, male/female                              | 102 (36.69%)/176 (63.31%) |
| Race/ethnicity  |                           |
| Hispanic  | 45 (16.19%)               |
| White   | 98 (35.25%)               |
| Black   | 122 (43.89%)              |
| Other   | 11 (3.96%)                |
| Missing   | 2 (0.72%)                 |
| Highest grade level   |                           |
| 12th grade or less (No diploma)                                 | 12 (4.32%)                |
| High school graduate or GED                                     | 77 (27.70%)               |
| Some college (No degree)  | 90 (32.37%)               |
| Associates degree (Occupational/Vocational or Academic program) | 31 (11.15%)               |
| Bachelor's degree   | 50 (17.99%)               |
| Graduate degree (Master's, Professional, or Doctoral)           | 18 (6.48%)                |
| Income level  |                           |
| <\$19,000   | 64 (23.02%)               |
| \$19,001–\$35,000   | 86 (30.94%)               |
| \$35,001–\$50,000   | 37 (12.31%)               |
| \$50,001–\$75,000   | 27 (9.71%)                |
| \$75,001–\$100,000  | 15 (5.40%)                |
| >\$100,000  | 21 (7.55%)                |
| Missing   | 28 (10%)                  |
| <i>Clinical characteristics</i>                                 |                           |
| PCL-5 scores  |                           |
| (30 days pre-ED) ( <i>n</i> = 201)                              | 30.76 (15.88)             |
| 2-week ( <i>n</i> = 244)  | 30.50 (17.14)             |
| 6-month ( <i>n</i> = 199)                                       | 22.17 (17.49)             |
| PROMIS depression   |                           |
| Prior (30 days pre-ED) ( <i>n</i> = 277)                        | 49.87 (10.71)             |
| 2-week ( <i>n</i> = 255)  | 55.63 (9.83)              |
| 6-month ( <i>n</i> = 197)                                       | 52.49 (10.47)             |
| LEC-5 scores ( <i>n</i> = 220)                                  | 10.49 (10.13)             |

### Magnetic resonance imaging

**General procedures.** MRI data were collected across five sites with harmonized acquisition parameters (Table S2). In the present analyses, we utilized participants' T1-weighted, DWI, task-fMRI during a threat reactivity task, and resting-state fMRI data. Results included in this manuscript come from preprocessing performed using FMRIPREP version stable 1.2.2, a Nipype-based tool [42, 43]. Details of the pipeline are described in the supplemental material. Modality and feature-specific processing are described below. A schematic of the overall processing and analytic steps are provided in the supplement (Figure S1).

### Voxel-based morphometry and surface-based morphology

T1-weighted MRI data were visually inspected and assessed using MRIQC [44]. We excluded participants based on coefficient of joint variation (CJV), a measure of motion and voxel non-uniformity, by a value of  $>2$  SD ( $n = 23$ ). Voxel-based morphometry (VBM) and cortical surface features were generated as in our prior reports [28, 33]. VBM was completed using standard FSL routines (i.e., FSLVBM) of the participants' anatomical scan [45–47]. Normalized and modulated gray matter volume (GMV) maps were smoothed using a 4 mm full-width at half-maximum (FWHM) Gaussian Kernel and re-masked by a participant-derived gray matter mask. The VBM

results were visually inspected and participants with poor segmentation were omitted ( $n = 24$ ) from the multimodal analysis. Cortical surface maps were reconstructed through FreeSurfer within the FMRIPREP framework [42, 43]. Individual participant maps of cortical thickness (CT) and pial surface area (PSA) were resampled into the fsaverage space and smoothed at a range of 10 mm FWHM.

### Diffusion tensor imaging (DTI)

DTI of the white matter skeleton was completed to derive metrics of white matter microstructure as described in our prior reports [28, 33]. Briefly, the processing pipeline was developed according to the recommendations of the ENIGMA consortium (<http://enigma.ini.usc.edu/protocols/dti-protocols/>). To ensure quality data, we calculated metrics of temporal signal-to-noise ratio and outlier maximum voxel intensity as in a prior report [47]. Participants who demonstrated both (a) TSNR values lower than 4.88 and (b) maximum voxel intensities  $>5000$  were removed from analyses to retain the maximum number of participants while removing low-quality data. Motion and eddy current effects in diffusion data were reduced using the 'eddy' subroutine in the FMRIB Software Library (FSL) [47–49] and susceptibility effects were corrected using nonlinear warping of the diffusion data to the participant's anatomical data [50]. Diffusion data were fit with a tensor model and Tract-Based Spatial Statistics (TBSS) processing was implemented following the ENIGMA-DTI working group processing standards to generate fractional anisotropy (FA), mean diffusivity (MD), and mode of the diffusion tensor (MO) skeletal maps [51, 52].

### Task-fMRI

To index neural reactivity to threat, participants completed an emotional reactivity task designed to probe reactivity to social threat cues via passive viewing of fearful and neutral facial expressions. The task is described in prior work [19, 23, 36]. Faces from the Ekman faces library were presented in a block design with 8 different faces of the same emotion (fear vs. neutral) within an 8 s block. Individual faces were presented for 500 ms each with a 500 ms interstimulus interval. Participants were given three 10 s rest periods evenly distributed throughout the task. The 5 min task included 15 fear blocks and 15 neutral blocks presented in a pseudorandom order. The order was counterbalanced across participants. The 1st-level models of these data were completed in SPM12 after denoising with ICA-AROMA as part of the FMRIPREP pipeline, which has been shown to handle motion artifacts in a robust, data-driven fashion that performs equal to and in some cases better than standard scrubbing or censoring procedures at the individual participant level [53–55]. Task blocks were modeled with separate boxcar functions representing the onset and 8000 ms duration of each block, convolved with a canonical hemodynamic response function. Separate regressors for white matter, cerebrospinal fluid, and global signal were included to account for any remaining motion/physiological noise following ICA. Group-level statistical modeling was completed in AFNI on the 1st level contrasts of fearful  $>$  neutral face contrast.

### Resting-state fMRI

Resting state fMRI data were further processed within the Analysis for Functional NeuroImages (AFNI) program 3dTproject following denoising with ICA-AROMA to perform linear detrending, censoring of non-steady state volumes identified by FMRIPREP, bandpass filtering (0.01–0.1 Hz), and regression of white matter, cerebrospinal fluid, and global signal to account for potential physiological noise. Group ICA via MELODIC was completed as described in our prior report [22]. Automatic dimensionality reduction selected 77 independent components. We focused the initial analyses on two RSNs based on our a priori hypotheses and findings from an earlier report: the default mode network and an amygdala-hippocampal functional covariance network [22]. Spatial maps of selected RSNs for analysis are depicted in the supplement (Figure S2). Exploratory analyses of additional spatial maps that covered visual and "arousal" regions seen in our prior work were also completed ( $n = 6$ ) [33]. Dual regression was performed to derive individual participant spatial maps for each component as described previously [22, 56, 57].

### Linked independent component analysis

Linked independent component analysis (LICA) was completed using FSL and MATLAB to perform multimodal data fusion [58, 59]. LICA leverages joint information reflected in the MR modalities to identify correlated patterns of structural and diffusion spatial variation that are linked

together through a subjects loading matrix reflecting the strength of the component pattern for each participant. Each identified component is thus composed of two parts: (1) a spatial map, for each modality, that describes regional variability that is related to variability to all other modalities and (2) participant loadings that describe an individual participant's relative strength of the component relative to all other participants. The FA, MD, MO, GMV, CT, and PSA maps from the 2-week MRI scan were used as spatial features. LICA was completed at a high dimensionality ( $L = 119$ , the maximum estimated within LICA) to better separate signal and noise (i.e., participant-dominated and motion) components [33, 59–61]. We specifically focused on identifying a component reflecting the ventral visual stream and thus only selected a single component for analyses to limit multiple comparisons. A subset ( $n = 83$ ) of participants had usable, longitudinal multimodal MRI data from an identical imaging session completed 6 months after trauma exposure. Components from the LICA performed with 2-week MRI data were projected to the 6-month data via multivariate spatial regression similar to the first stage of dual regression, for each modality separately [61] to derive a set of subject loadings for each modality. The loadings were then averaged together to generate an estimated 6-month component loading.

### Statistical analyses

Statistical analyses were completed using IBM SPSS version 24, the JASP Statistical Package (<https://jasp-stats.org/>), and the Analysis of Functional NeuroImages (AFNI) software package [62]. We completed multiple linear regressions to evaluate if SCN loadings were associated with acute (i.e., 2-week) PTSD symptoms. Regressions included dummy-coded scanner and sex assigned at birth covariates as well as continuous covariates for age at enrollment, pre-trauma PTSD symptoms reported in the ED, and total score on the LEC-5. Linear and quadratic predictors of 2-week PTSD from the PCL-5 were included. The model was chosen to harmonize with our previously reported approach [33]. Inclusion of the prior PTSD symptoms and LEC-5 scores reduced the sample size for analyses and thus we also completed the regressions removing these covariates. In the prior report, we observed a positive relationship between VVS SCN loadings and PTSD symptoms, with some specificity for re-experiencing symptoms and thus we anticipated a similar effect in the present analyses. Given our a priori hypothesis on the association between 2-week SCN loadings and PCL-5 scores, we set a nominal  $p$ -value of 0.05 with one-tailed testing for the model with a Bonferroni–Holm correction to account for the multiple comparisons (models with and without covariates). Similar models were completed for estimated 6-month SCN loadings, however, the quadratic term was removed given findings from the previous models (described in the “Results”). Given the lack of a directional hypothesis for these sets of tests, we set a nominal  $p$ -value 0.05 with two-tailed testing for the models and a Bonferroni–Holm correction was applied for each set (i.e., with and without covariates) of models. Significant associations with total PTSD symptom severity in the above models were followed-up with identical models substituting PTSD subscale scores to understand the domains driving the effect. For models with a significant subscale association with SCN loadings, we compared standardized regression coefficients between the significant model and all other models using a  $Z$ -test [63]. We further completed repeated-measures analysis of covariance (RM-ANCOVA) to assess the effect of changes in component loadings on PCL-5 scores (dependent variable) with a within-subject's factor for time (2 weeks and 6 months), a continuous measure of change in VVS SCN loadings (6-month minus 2-week), and covariates for age, sex assigned at birth, and scanner site. We also completed multiple regressions to assess the relationship between 2-week component loadings and Clinician Administered PTSD Scale for DSM-IV (CAPS-IV) nightmare frequency, intensity, and severity (3 separate models) while covarying for scanner site, age, and sex assigned at birth. A Bonferroni–Holm correction was applied to the models of nightmare symptoms to account for multiple comparisons. We present only a priori outcomes of interest from regression models in the results, but full outputs are available in the supplement. Voxelwise group-level models of the resting state fMRI data were completed using `3dttest++` in AFNI for the default mode and amygdala-hippocampal functional covariance networks (two separate models). Models included a continuous regressor of loadings from the ventral visual stream SCN as well as covariates for scanner, age, and sex assigned at birth. A gray matter mask that included subcortical areas and the cerebellum was applied to the data. Permutation-based cluster correction (i.e., the `-clustsim` option in `3dttest++`) was used to determine the corresponding voxel extent  $k$  needed at a cluster forming threshold of  $p = 0.005$  to maintain  $\alpha = 0.05$

(10,000 iterations). Cluster-corrected results were considered significant at a corrected  $p < 0.025$  to account for the two networks assessed. A separate voxelwise comparison was completed for the threat reactivity task. Given that the present study used pooled, multisite data, we completed supplementary assessments of data quality between each site and these analyses are documented in the supplementary material (Figure S2).

## RESULTS

### Participant demographics

Participant demographics are presented in Table 1. Correlations between the psychometric instruments are presented in Table 2. Indices of PTSD and depression were correlated at each timepoint, and these were in turn related to CAPS-IV nightmare frequency, intensity, and severity. Independent samples  $t$ -tests did not reveal a significant difference in PCL-5 scores between participants who did or did not provide 6-month MRI data either at 2 weeks [ $t(242) = 1.27, p = 0.207$ ] or 6 months [ $t(197) = -0.21, p = 0.831$ ]. Thus the present data come from a largely female, racially/ethnically diverse sample with varying degrees of posttraumatic dysfunction.

### Structural covariance of the ventral visual stream is associated with acute posttraumatic dysfunction

LICA revealed a structural covariance network (SCN) of the ventral visual stream (VVS) associated with acute PTSD severity (PCL-5 scores) (Fig. 1; Table S3). The SCN primarily reflected fractional anisotropy (FA; 20%), gray matter volume (GMV; 23%), and pial surface area (PSA; 20%) of the inferior fronto-occipital fasciculus, visual cortex, and anterior temporal pole (i.e., bilateral medial aspects of the ventral visual stream; VVS). In line with our a priori hypothesis, loadings on the SCN were significantly linearly associated with PTSD symptoms at 2 weeks, with [ $t(133) = 1.98, \beta = 0.22, 95\% \text{ CI} = [0.02, 0.42], p_{\text{corrected}} = 0.05, \text{ one-tailed}$ ] and without [ $t(235) = 1.77, \beta = 0.13, 95\% \text{ CI} = [-0.01, 0.27], p_{\text{corrected}} = 0.04, \text{ one-tailed}$ ] the inclusion of covariates for prior trauma history (LEC-5 total score) and pre-trauma PTSD symptoms. Given the prior findings, we assessed if the associations were specific to individual PTSD symptom dimensions (indexed by PCL-5 subscale scores). Loadings on the SCN were significantly linearly associated with intrusion symptoms (e.g., flashbacks, re-experiencing, etc.) [ $t(133) = 2.16, \beta = 0.23, 95\% \text{ CI} = [0.01, 0.45], p = 0.033$ ], but not avoidance, negative cognition/mood, or arousal symptoms (all  $p > 0.05$ ). Comparison of  $\beta$ -values revealed the association between the SCN loadings and intrusion symptoms was significantly different compared to the association with avoidance ( $Z$ -value = 2.30,  $p = 0.022$ ), negative alterations in cognition and mood ( $Z$ -value = 2.62, 0.009), and arousal ( $Z$ -value = 2.54,  $p = 0.011$ ) subscales. We further completed supplementary analyses to determine if similar associations were observed between VVS SCN loadings and depression symptoms (using the PROMIS). We did not observe any linear or curvilinear associations between VVS SCN loadings and depressive symptoms with or without accounting for prior trauma or pre-trauma PTSD symptoms (Table S4). These data replicate prior observations of a positive association between VVS SCN loadings and re-experiencing symptoms in a smaller sample [33] and suggest structural covariance of the VVS is positively related to intrusive memories in the aftermath of traumatic stress.

Given the potential visual representation of traumatic memories experienced in nightmares for individuals with PTSD [64], we completed additional analyses to directly assess if the SCN was related to nightmare experiences in the early aftermath of trauma (Fig. 2; Table S5). SCN loadings were linearly associated with 2-week nightmare severity [ $t(245) = 2.41, \beta = 0.15, 95\% \text{ CI} = [0.02, 0.28], p_{\text{corrected}} = 0.034$ ] and intensity [ $t(245) = 2.64, \beta = 0.17, 95\% \text{ CI} = [0.04, 0.30], p_{\text{corrected}} = 0.027$ ], but not frequency [ $t(245) = 1.81, \beta = 0.12, 95\% \text{ CI} = [-0.01, 0.25], p_{\text{corrected}} = 0.071$ ].

**Table 2.** Psychometric variable correlations.

| Variables                       | PCL-5 (prior) | PCL-5 (2 weeks) | PCL-5 (6 months) | PROMIS depression (prior) | PROMIS depression (2 weeks) | PROMIS depression (6 months) | LEC-5 (total score) | Nightmare frequency | Nightmare intensity |
|---------------------------------|---------------|-----------------|------------------|---------------------------|-----------------------------|------------------------------|---------------------|---------------------|---------------------|
| 1. PCL-5 (2 weeks)              | 0.524** (177) |                 |                  |                           |                             |                              |                     |                     |                     |
| 2. PCL-5 (6 months)             | 0.492** (145) | 0.507** (185)   |                  |                           |                             |                              |                     |                     |                     |
| 3. PROMIS Depression (prior)    | 0.532** (200) | 0.360** (243)   | 0.303** (198)    |                           |                             |                              |                     |                     |                     |
| 4. PROMIS Depression (2 weeks)  | 0.446** (186) | 0.757** (244)   | 0.429** (191)    | 0.524** (254)             |                             |                              |                     |                     |                     |
| 5. PROMIS Depression (6 months) | 0.387** (144) | 0.410** (184)   | 0.804** (193)    | 0.428** (196)             | 0.504** (190)               |                              |                     |                     |                     |
| 6. LEC-5 (total score)          | 0.066 (158)   | 0.193** (203)   | 0.115 (177)      | 0.138* (219)              | 0.119 (213)                 | 0.087 (174)                  |                     |                     |                     |
| 7. Nightmare Frequency          | 0.325** (185) | 0.487** (243)   | 0.330** (190)    | 0.191** (252)             | 0.383** (253)               | 0.220** (189)                | -0.046 (212)        |                     |                     |
| 8. Nightmare intensity          | 0.293** (185) | 0.490** (243)   | 0.373** (190)    | 0.178** (252)             | 0.365** (253)               | 0.253** (189)                | 0.01 (212)          | 0.729** (253)       |                     |
| 9. Nightmare severity           | 0.333** (185) | 0.525** (243)   | 0.375** (190)    | 0.198** (252)             | 0.402** (253)               | 0.252** (189)                | -0.019 (212)        | 0.926** (253)       | 0.933** (253)       |

\* $p < 0.05$ , \*\* $p < 0.01$ , PCL-5 = PTSD Checklist for DSM-5; PROMIS = Patient-Reported Outcomes Measurement Information System. Data presented as  $r$ -value ( $n$ ).

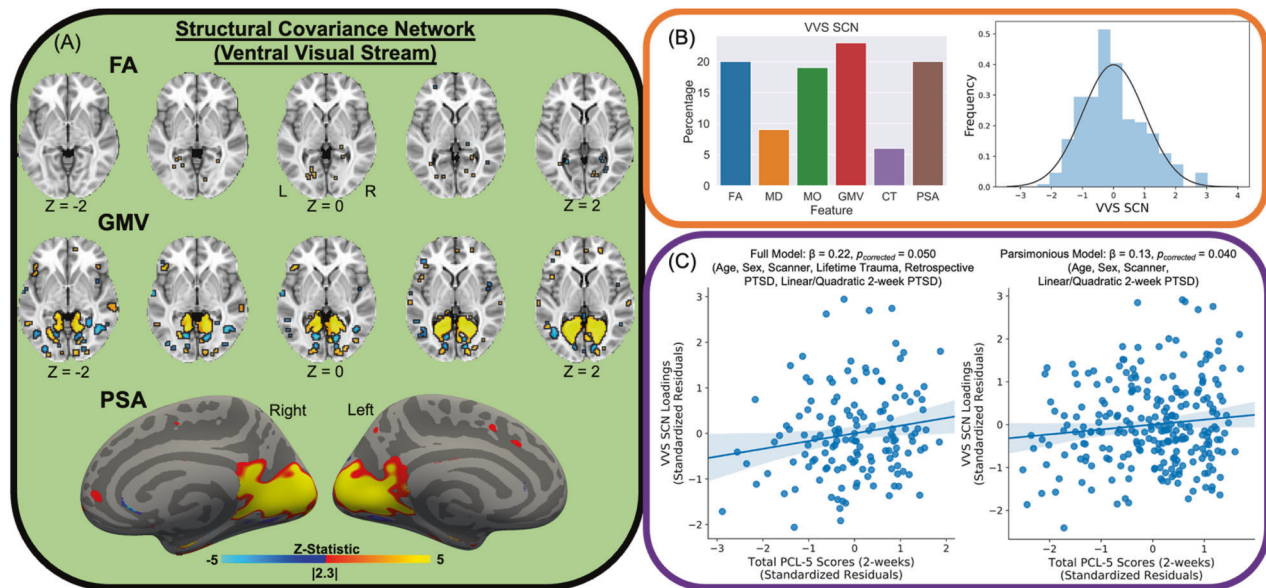


**Fig. 1** Structural covariance network of the ventral visual stream and acute PTSD severity. Linked independent components analysis (LICA) was completed on fractional anisotropy (FA), mean diffusivity (MD), mode of the diffusion tensor (MO), gray matter volume (GMV), cortical thickness (CT), and pial surface area (PSA) spatial maps to derive multimodal components. We observed a component that reflected a structural analog of the ventral visual stream derived from all participants (A). The component predominantly reflected FA, GMV, and PSA of the visual cortex, anterior temporal lobe, and the inferior fronto-occipital fasciculus (left) and the distribution of loadings across participants (right) (B). The component was related to total scores on the PTSD Checklist for DSM-5 (PCL-5) in both full (left) and parsimonious (right) models described in the “Methods” section (C). Brain figures represent the ventral visual stream structural covariance network obtained from LICA across all participants. Scatter plots are partial plots where dots represent the standardized residuals of individual participant loadings and PCL-5 scores. Lines represent the linear line of best fit and the shaded bar represents the 95% confidence interval.

In line with the prior analyses, these data suggest that structural covariance of the VVS may be particularly related to traumatic visual memory encoding, retrieval, and expression.

### Structural covariance of the ventral visual stream moderates amygdala-hippocampal to inferior temporal gyrus connectivity

Greater loadings of the VVS SCN were negatively related to resting-state functional connectivity between an amygdala-hippocampal RSN and the inferior temporal gyrus, a component of the VVS [ $Z_{Peak} = -3.87$ ,  $p_{corrected} < 0.02$ ,  $k = 61$  (488 mm<sup>3</sup>), (XYZ = 52, -65, -7)] (Fig. 3). No other significant associations between VVS SCN loadings and resting-state connectivity were observed, even for RSNs that overlapped the VVS. No significant effects of VVS SCN loadings on amygdala reactivity to threat (fearful – neutral) were observed. These findings suggest structural covariance of the VVS impacts connectivity between the arousal network and components of the VVS.

### Future ventral visual stream structural covariance and posttraumatic stress symptoms

Prior to analysis of the 6-month imaging data, we assessed if the VVS SCN loadings at 2 weeks were related to participants’ 6-month PTSD symptoms. The regression models included linear and quadratic terms for 6-month PTSD symptoms, and covariates for scanner, age, and participant sex assigned at birth. A separate model also included additional covariates for prior trauma history and PTSD symptoms (i.e., prior to admission to the ED). No significant associations between the 2-week VVS SCN loadings and 6-month PTSD symptoms were observed (all  $p > 0.05$ ).

The SCN for the VVS was then projected onto participants’ 6-month MRI data to assess relationship between VVS SCN loadings and PTSD symptoms over time (Fig. 4; Table S6). In contrast to the positive association identified with 2-week loadings, VVS SCN loadings at 6 months were negatively associated with PTSD symptoms at 2 weeks [ $t(68) = -2.45$ ,

$\beta = -0.27$ , 95% CI = [−0.45, −0.09],  $p_{corrected} = 0.034$ ], however, the association was not significant when covarying for prior trauma history and pre-trauma PTSD symptoms [ $t(32) = -0.58$ ,  $\beta = -0.12$ , 95% CI = [−0.62, 0.38],  $p_{corrected} = 0.564$ ]. Further, VVS SCN loadings at 6 months were negatively associated with PTSD symptoms at 6 months [ $t(72) = -2.53$ ,  $\beta = -0.27$ , 95% CI = [−0.45, −0.09],  $p_{corrected} = 0.026$ ]. The effect was not significant when covarying for prior trauma history and pre-trauma PTSD symptoms [ $t(35) = -1.23$ ,  $\beta = -0.26$ , 95% CI = [−0.73, 0.25],  $p_{corrected} = 0.229$ ]. We also completed analyses to assess if there was a relationship between SCN loadings and individual PTSD symptom dimensions (indexed by PCL-5 subscale scores). At 6 months, SCN loadings were negatively associated with 6-month negative cognition and mood symptoms [ $t(72) = -2.40$ ,  $\beta = -0.26$ , 95% CI = [−0.48, −0.07],  $p = 0.019$ ], but not intrusion, avoidance, or arousal symptoms (all  $p > 0.05$ ). Comparison of  $\beta$ -values revealed the association between the SCN loadings and negative alterations in cognition and mood symptoms was significantly different compared to the association with intrusion (Z-value = 2.36,  $p = 0.018$ ), avoidance (Z-value = 2.23, 0.026), and arousal (Z-value = 2.13,  $p = 0.034$ ) subscales. These findings suggest that, while greater structural covariance of the VVS facilitates encoding of traumatic memories acutely after trauma, decreased structural covariance over time contributes to negative trauma-related thoughts and feelings.

Together, the prior findings suggested that individuals at risk for greater PTSD symptoms showed relatively high structural integrity within the VVS early posttrauma, but also showed lower VVS integrity in the future. We completed a follow-up RM-ANCOVA to directly investigate associations between change over time in the VVS and PTSD symptoms. Although we did not observe a significant time by change in VVS SCN loadings interaction on PTSD symptoms [ $F(1,66) = 0.51$ ,  $p = 0.480$ ], the RM-ANCOVA revealed a significant effect of change in VVS SCN loadings on PTSD symptoms [ $F(1,66) = 8.82$ ,  $p = 0.004$ ]. Follow-up linear regressions revealed that decreased loadings over time were

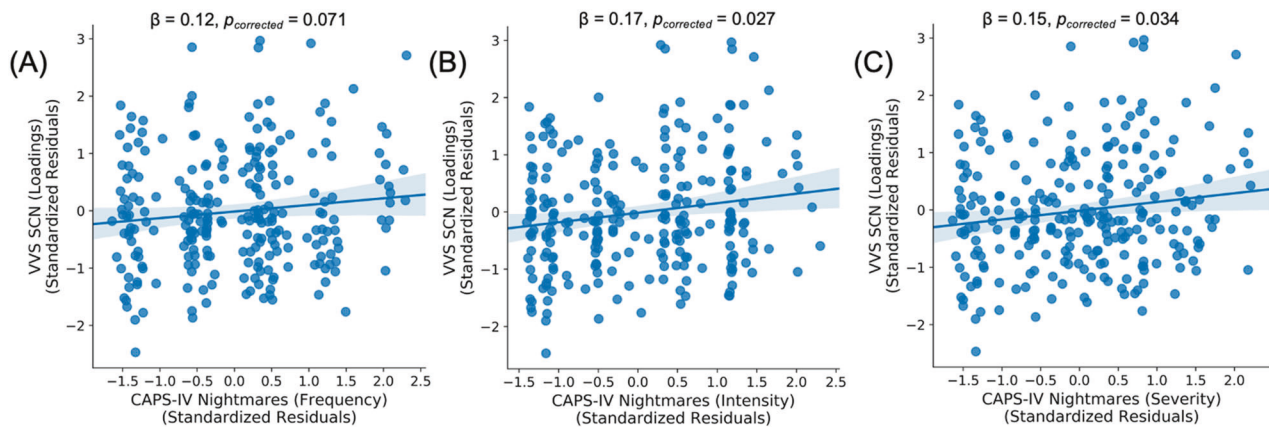


**Fig. 2 Ventral visual stream structural covariance strength is related to nightmare symptoms.** Individual participant loadings on the VVS SCN identified through linked independent components analysis (LICA) varied positively with participants' nightmare frequency (A), intensity (B), and severity (C) scores at 2 weeks post trauma. Scatter plots are partial plots where dots represent the standardized residuals of individual participant loadings and nightmare index scores. Lines represent the linear line of best fit and the shaded bar represents the 95% confidence interval.

associated with greater PTSD symptoms [ $t(66) = -2.97$ ,  $\beta = -0.36$ , 95% CI =  $[-0.60, -0.12]$ ,  $p = 0.004$ ]. Of note, a follow-up paired-samples  $t$ -test of 2-week versus 6-month VVS SCN loadings did not reveal a significant difference [ $t(82) = 0.28$ ,  $p = 0.781$ ]. These data indicate individuals with high structural integrity within the ventral visual system in the early week post-trauma, and who lose this integrity over time, are most at risk for persistent PTSD-related dysfunction.

## DISCUSSION

Multivariate MRI approaches hold promise for identifying neural signatures of susceptibility to trauma and stress-related disorders. However, limited work has investigated potential multivariate neural signatures of visual circuitry structure in recently traumatized individuals. In the current report, representing one of the largest prospective and longitudinal neuroimaging studies of trauma survivors, we identified a multimodal structural covariance network (SCN) of the ventral visual stream that is spatially consistent with our prior observations [33]. Loadings on the ventral visual stream SCN, 2 weeks post trauma exposure, were positively associated with 2-week PTSD symptoms. The SCN was also associated with both 2-week intrusion and nightmare symptoms. Further, loadings on the SCN varied with connectivity between the amygdala/hippocampus and inferior temporal gyrus which is part of the VVS. Interestingly, estimated loadings of the ventral visual stream SCN at 6 months were negatively associated with 6-month PTSD symptoms and individuals who showed decreased strength of the VVS SCN over time generally had higher PTSD symptoms. These findings provide multidimensional evidence of a role for the structure of the ventral visual stream in both the development and course of PTSD symptoms.

Multimodal data fusion via linked independent components analysis revealed an SCN that reflected white matter microstructure and gray matter morphology of the visual cortex, inferior fronto-occipital fasciculus, inferior temporal gyrus, and anterior temporal lobe (i.e., the ventral visual stream). The ventral visual stream is intimately involved in recognition of objects, their properties, and their representative meanings [12, 13] and is critical for processing of affective visual stimuli [9, 65, 66]. Importantly, the ventral visual stream may also be directly involved in memory retrieval processes for high arousal, threatening stimuli [67, 68]. In the present study, loadings on the ventral visual stream SCN were positively associated with acute (i.e., 2 weeks) PTSD symptoms. Given the positive loadings

on the SCN reflected greater gray matter volume and pial surface area of visual stream regions, and the resulting positive association between SCN loadings and PTSD symptoms, it may be that greater structural integrity of the ventral visual stream in the early aftermath of trauma contributes to greater attention and reactivity to potentially threat-related visual stimuli. In turn, the network may facilitate encoding or consolidation of a threat-relevant visual memory. Enhanced neural ability to form strong visual memories may lead to stronger and more enduring trauma-related memories that ultimately contribute to the enhanced PTSD symptoms observed in the sample. Of note, our follow-up analyses revealed 2-week associations with the ventral visual stream SCN were more strongly related to intrusion symptoms consistent with our prior findings [33]. Thus, as opposed to increased consolidation, it may be that greater integrity of the network facilitates enhanced retrieval of the trauma-related threat memory and efficient reactivation of visual components of the trauma memory thereby exacerbating PTSD symptoms. The present findings cannot dissociate either the potential for enhanced consolidation or enhanced retrieval, nor can they rule out that both processes are acting in tandem in those with greater structural covariance of the ventral visual stream. We note, though, a possibility that the present results are unrelated to threat-processing and reflect a more domain-general process such that greater covariance could contribute to appetitive or highly salient memories regardless of valence. Future work should thus investigate threat and non-threat processing of the ventral visual stream in trauma-exposed individuals to better understand how the function of this circuitry is linked to PTSD.

Individual variability in the ventral visual stream SCN was positively associated with nightmare intensity. Though often overlooked, sleep disturbances are frequent and distressing consequences for trauma victims [8, 69–71]. Nightmare experiences are particularly damaging as they can contribute to negative emotional states and maladaptive behaviors in trauma victims [72–74]. It is possible, given the role of the ventral visual stream in emotion and determining representational meaning, that the observed association may be related to consolidation of trauma-related memories that may occur during sleep in line with our hypothesis above [75]. Individuals susceptible to posttraumatic nightmares may also be susceptible to more enduring but generalizable visual trauma memories which are in turn facilitated by the greater structural integrity of the ventral visual stream. However, it is not necessarily the case that the nightmares experienced by participants here are directly related to their

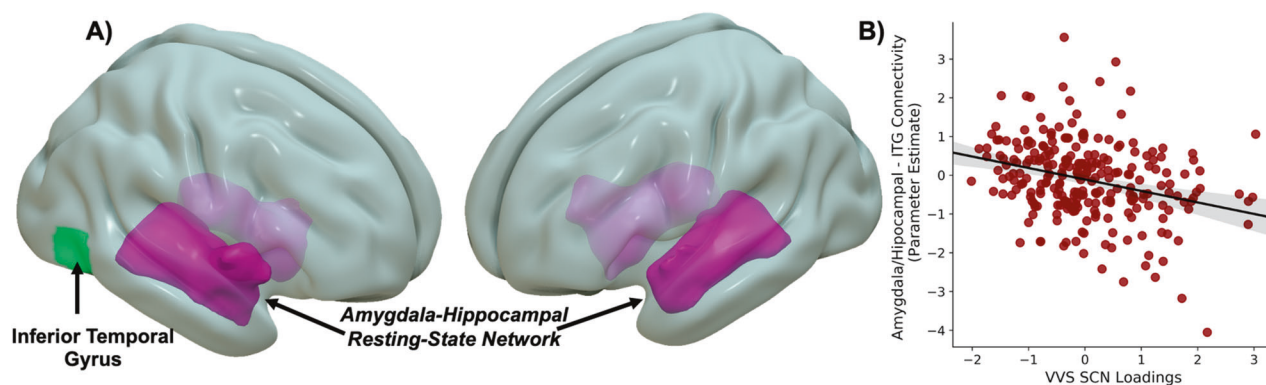


**Fig. 3 Ventral visual stream structural covariance strength is associated with arousal network connectivity to inferior temporal gyrus.** We observed that strength of a structural covariance network of the ventral visual stream modulated connectivity between an amygdala-hippocampal functional covariance network and inferior temporal gyrus (A) such that greater structural covariance network loadings were associated with negative connectivity (B). Scatter plots are full plots where dots represent individual participant linked independent components analysis component loadings and parameter estimates of amygdala/hippocampal to inferior temporal gyrus connectivity. Lines represent the linear line of best fit and the shaded bar represents the 95% confidence interval.

traumatic event. Future work is needed to fully understand the relationship between posttraumatic nightmares and visual processing circuitry.

Loading strength of the ventral visual stream SCN was associated with amygdala-hippocampal connectivity to the inferior temporal gyrus (ITG). We recently demonstrated that “arousal network” to dorsolateral PFC as well as default mode to ITG connectivity was related to 3-month PTSD symptoms within the AURORA study [22]. The ITG cluster we observed in the present report showed high spatial overlap to that in the previous report with a similar central locus of the effect. The ITG is part of the anterior ventral visual stream and may support both high-level visual modeling and threat-specific processing as part of the ventral visual stream [76, 77]. In the present sample, greater structural covariance was associated with negative connectivity between the arousal network and ITG. The findings suggest that, in individuals with higher structural covariance of the ventral visual stream, arousing or salient contexts of stimuli are not properly integrated during encoding or retrieval of representative visual information regarding trauma cues. The suggested dysfunctional affective-visual encoding process may, in turn, be related to generalization of threat memories that characterize PTSD. This speculative process fits with the additional finding that greater loadings on the ventral visual stream SCN were associated with greater expression of acute PTSD symptoms. It may thus be somewhat surprising, given this interpretation, that no association was observed between SCN loadings and neural reactivity to threat indexed via a fearful face viewing task. The threat reactivity task has been used in several studies and shows pronounced activation of the amygdala and visual cortex, and it is associated with both acute and chronic posttraumatic dysfunction [20, 23, 36]. However, it is important to note that the present task involved passive viewing of stimuli without a requirement for participants to encode stimulus information such as valence. Given the previously described associations with intrusion symptoms, it may be that tasks that more explicitly involve emotional memory processes (e.g., Pavlovian threat conditioning) may show more robust associations with the ventral visual stream SCN. Together, these data suggest that amygdala-hippocampal connectivity with the posterior ventral visual stream may facilitate encoding of threat-relevant visual cues that ultimately contributes to PTSD susceptibility.

Of note, associations between ventral visual stream SCN loadings and PTSD symptoms were not stable between the 2-week and 6-month assessment timepoints. Thus, it may be that trauma-exposed participants’ ventral visual stream covariance

represents a brain state that is unique in the immediate aftermath of, but changes over the 6 months following, trauma. Although 2-week ventral visual stream SCN loadings were positively associated with 2-week PTSD symptoms, we found ventral visual stream SCN loadings at 6 months were negatively associated with 6-month PTSD symptoms. Relatedly, individuals who showed decreases in SCN loadings over time also showed greater average PTSD symptoms at 6 months. The association between SCN loadings and acute posttraumatic symptoms was also strengthened when accounting for prior trauma and PTSD symptoms indicating a potential specificity of ventral visual stream integrity to stress reactivity in the early aftermath of trauma. These findings suggest that PTSD symptoms are associated with initially high, but then weakened, structural integrity of the ventral visual stream.

One way to conceptualize the present data is within a framework of delayed excitatory neurotoxicity effects of traumatic stress on brain structure. Acute stressors lead to selective neurogenesis and synaptic strengthening of circuits critical for formation of threat-relevant memories in animal models [78–80]. In humans, acute stress facilitates threat learning but contributes to overgeneralization which is further observed after trauma and in those with PTSD [81–83]. Threat-memory formation is highly glutamate-dependent, particularly within prefrontal-hippocampal circuitry, and dysregulated glutamatergic activity can lead to neural cell death and diminished gray matter volume [79, 84–86]. Thus, although acute stress can facilitate threat learning, supported by greater integrity of associated neural circuitry, chronic stress may lead to degeneration of the circuitry and contribute to delayed threat processing dysfunction. It may be that the chronic stress and potentially chronic activity of the ventral visual stream some individuals may experience following acute trauma have a deleterious effect on structural integrity of the visual pathway contributing to the differential associations. An interesting hypothesis for future testing relates to whether this apparent decreased visual stream structural integrity may contribute to generalization of visual threat cues seen in chronic PTSD. This framework may also help to explain dissociative findings in samples of recent trauma victims that show greater prefrontal glutamate/glutamine concentrations and null/mixed associations between brain volume and PTSD [30, 87, 88] compared to chronic PTSD samples [89–91].

Several limitations should be considered when interpreting the present findings. The present approach required participants to have complete MRI data across a number of features which reduced our sample size. It is important to note that participants

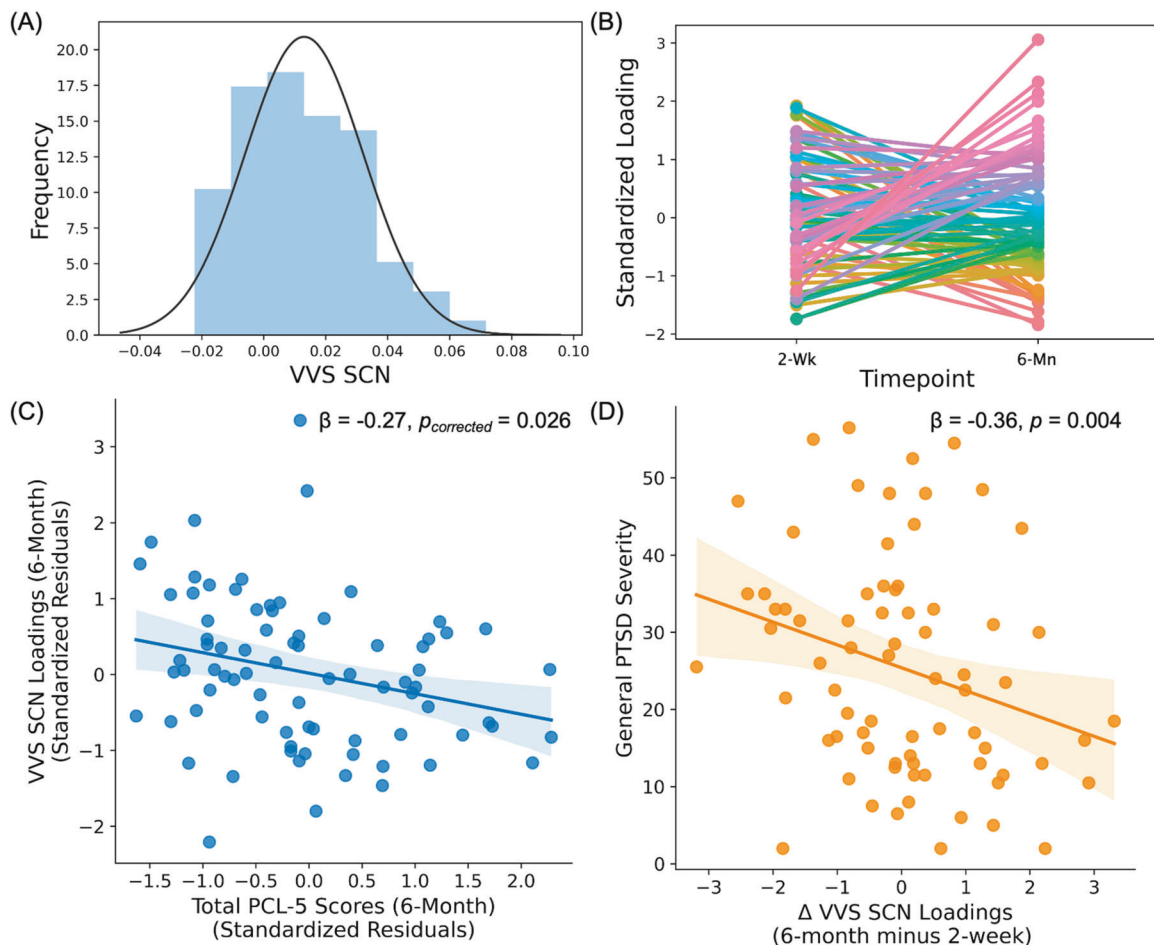


**Fig. 4 Stability of ventral visual stream structural covariance network over time.** Similar to structural covariance network (SCN) loadings at 2 weeks, the 6-month loadings on component 21 were largely normally distributed (A). Individuals showed variability in component loadings between timepoint 1 (i.e., 2 weeks) and timepoint 2 (i.e., 6 months) post-trauma (B). The component loadings at 6 months were related to total scores on the PTSD Checklist for DSM-5 (PCL-5) at 6 months in models described in the “Methods” section (C). Participants who showed an overall decrease in SCN loadings over time showed greater PTSD symptom severity over time than those with increased SCN loadings (D). Scatter plots are partial plots where dots represent the standardized residuals of individual participant loadings and PCL-5 scores. Lines represent the linear line of best fit and the shaded bar represents the 95% confidence interval.

who completed all MRI scans and had higher quality data may be phenotypically different from those who did not and these factors may be relevant for PTSD symptomatology. Thus, it is unclear if these data are generalizable to participants who drop out of research studies—who may in fact be most at risk for developing PTSD after trauma. It is also worth noting that, although we observed unique associations between VVS SCN loadings and specific PTSD symptom dimensions at 2 weeks and 6 months, such symptom dimensions are highly correlated with one another. Although we completed additional analyses with nightmare symptoms, additional data that assess psychological processes related to specific PTSD symptom dimensions (e.g., sensory sensitivity, memory consolidation strength, physiological reactivity) collected concurrently with MRI data may provide further support for the present findings. Another limitation is the lack of a non-trauma-exposed sample. Inclusion of a non-trauma sample is difficult given the preponderance of trauma in the U.S. (thereby questioning the ecological validity of the term “non-trauma”) and such a sample was excluded from AURORA due to feasibility constraints. Regardless, it remains unclear if trauma exposure itself may modulate the VVS SCN or if these would be observed in a non-trauma sample. Future work should investigate the occurrence and stability of a ventral visual stream SCN in non-trauma-exposed groups.

Our findings emphasize the often-overlooked role of sensory and particularly visual cortices in PTSD susceptibility after trauma. Further, the present data highlight potentially important relationship between the neural substrates of visual information processing and core threat neurocircuitry (e.g., amygdala/hippocampus) for understanding the development of PTSD. The current results also replicate prior findings in the largest-of-its-kind multisite, multimodal imaging study of recent trauma. Thus, modulation of visual neural circuitry after trauma opens new avenues for future research and potential neuromodulation techniques to reduce PTSD symptoms and nightmares in the aftermath of trauma [92–94]. Uncovering the nature of interactions between canonical threat and visual processing circuitry may provide the most effective avenue for the identification of robust and generalizable neural signatures of trauma and stress-related disorders.

#### DATA AVAILABILITY

Data and/or research tools used in the preparation of this manuscript were obtained from the National Institute of Mental Health (NIMH) Data Archive (NDA). NDA is a collaborative informatics system created by the National Institutes of Health to provide a national resource to support and accelerate research in mental health. Dataset identifier(s): NIMH Data Archive Digital Object Identifier 10.15154/1526071. This manuscript reflects the views of the authors and may not reflect the opinions or views of the NIH or of the Submitters submitting original data to NDA.

## CODE AVAILABILITY

Code for the present study was obtained as part of publicly available distributions of fMRIPREP (described in "Methods" and supplement), FSL, and AFNI. Commercial software was used in statistical analysis. Detailed code is available upon request.

## REFERENCES

- American Psychiatric Association. Diagnostic and statistical manual of mental disorders. 5th ed. 2013. <https://doi.org/10.1176/appi.books.9780890425596.744053>.
- Harnett NG, Goodman AM, Knight DC. PTSD-related neuroimaging abnormalities in brain function, structure, and biochemistry. *Exp Neurol*. 2020;330. <https://doi.org/10.1016/j.expneurol.2020.113331>.
- Bryant RA, Harvey AG. Visual imagery in posttraumatic stress disorder. *J Trauma Stress*. 1996;9:613–9.
- Fani N, King TZ, Clendinen C, Hardy RA, Surapaneni S, Blair JR, et al. Attentional control abnormalities in posttraumatic stress disorder: functional, behavioral, and structural correlates. *J Affect Disord*. 2019;253:343–51.
- Fani N, Jovanovic T, Ely TD, Bradley B, Gutman D, Tone EB, et al. Neural correlates of attention bias to threat in post-traumatic stress disorder. *Biol Psychol*. 2012;90:134–42.
- Fani N, Tone EB, Phifer J, Norrholm SD, Bradley B, Ressler KJ, et al. Attention bias toward threat is associated with exaggerated fear expression and impaired extinction in PTSD. *Psychological Med*. 2012;42:533–43.
- Brewin CR. Re-experiencing traumatic events in PTSD: new avenues in research on intrusive memories and flashbacks. *Eur J Psychotraumatol*. 2015;6. <https://doi.org/10.3402/ejpt.v6.27180>.
- Richards A, Kanady JC, Neylan TC. Sleep disturbance in PTSD and other anxiety-related disorders: an updated review of clinical features, physiological characteristics, and psychological and neurobiological mechanisms. *Neuropsychopharmacology*. 2020;45:55.
- Pessoa L, Adolphs R. Emotion processing and the amygdala: from a "low road" to "many roads" of evaluating biological significance. *Nat Rev Neurosci*. 2010;11:773–82.
- Hendler T, Rotshtein P, Yeshurun Y, Weizmann T, Kahn I, Ben-Bashat D, et al. Sensing the invisible: differential sensitivity of visual cortex and amygdala to traumatic context. *Neuroimage*. 2003;19:587–600.
- Mueller-Pfeiffer C, Schick M, Schulte-Vels T, O'Gorman R, Michels L, Martin-Soelch C, et al. Atypical visual processing in posttraumatic stress disorder. *NeuroImage: Clin*. 2013;3:531–8.
- Konkle T, Caramazza A. Tripartite organization of the ventral stream by animacy and object size. *J Neurosci*. 2013;33:10235–42.
- Long B, Yu CP, Konkle T. Mid-level visual features underlie the high-level categorical organization of the ventral stream. *Proc Natl Acad Sci USA*. 2018;115:E9015–E9024.
- Konkle T, Alvarez GA. A self-supervised domain-general learning framework for human ventral stream representation. *Nat Commun*. 2022;13:1–12.
- Kravitz DJ, Saleem KS, Baker CI, Ungerleider LG, Mishkin M. The ventral visual pathway: an expanded neural framework for the processing of object quality. *Trends Cogn Sci*. 2013;17:26–49.
- Rosen ML, Amso D, McLaughlin KA. The role of the visual association cortex in scaffolding prefrontal cortex development: a novel mechanism linking socioeconomic status and executive function. *Developmental Cogn Neurosci*. 2019;39:100699.
- Yoshii T, Oishi N, Ikoma K, Nishimura I, Sakai Y, Matsuda K, et al. Brain atrophy in the visual cortex and thalamus induced by severe stress in animal model. *Sci Rep*. 2017;7. <https://doi.org/10.1038/S41598-017-12917-Z>.
- Shackman AJ, Maxwell JS, McMenamin BW, Greischar LL, Davidson RJ. Stress potentiates early and attenuates late stages of visual processing. *J Neurosci*. 2011;31:1156.
- Stevens JS, Kim YJ, Galatzer-Levy IR, Reddy R, Ely TD, Nemeroff CB, et al. Amygdala reactivity and anterior cingulate habituation predict posttraumatic stress disorder symptom maintenance after acute civilian trauma. *Biol Psychiatry*. 2017;81:1023–9.
- McLaughlin KA, Busso DS, Duys A, Green JG, Alves S, Way M, et al. Amygdala response to negative stimuli predicts PTSD symptom onset following a terrorist attack. *Depress Anxiety*. 2014;31:834–42.
- Belleau EL, Ehret LE, Hanson JL, Brasel KJ, Larson CL, deRoon-Cassini TA. Amygdala functional connectivity in the acute aftermath of trauma prospectively predicts severity of posttraumatic stress symptoms: functional connectivity predicts future PTSD symptoms. *Neurobiol Stress*. 2020;12:100217.
- Harnett NG, van Rooij SJH, Ely TD, Lebois LAM, Murty VP, Jovanovic T, et al. Prognostic neuroimaging biomarkers of trauma-related psychopathology: resting-state fMRI shortly after trauma predicts future PTSD and depression symptoms in the AURORA study. *Neuropsychopharmacology*. 2021;46:1263–71.
- Stevens JS, Jovanovic T, Fani N, Ely TD, Glover EM, Bradley B, et al. Disrupted amygdala-prefrontal functional connectivity in civilian women with posttraumatic stress disorder. *J Psychiatr Res*. 2013;47:1469–78.
- Dark HE, Harnett NG, Knight AJ, Knight DC. Hippocampal volume varies with acute posttraumatic stress symptoms following medical trauma. *Behav Neurosci*. 2021;135:71–78.
- Koch SB, van Ast VA, Kaldewaj R, Hashemi MM, Zhang W, Klumpers F, et al. Larger dentate gyrus volume as predisposing resilience factor for the development of trauma-related symptoms. *Neuropsychopharmacology*. 2021;46:1283–92.
- Weis CN, Huggins AA, Miskovich TA, Fitzgerald JM, Bennett KP, Krukowski JL, et al. Acute white matter integrity post-trauma and prospective posttraumatic stress disorder symptoms. *Front Hum Neurosci*. 2021;15:582.
- Harnett NG, Ference EW, Knight AJ, Knight DC. White matter microstructure varies with post-traumatic stress severity following medical trauma. *Brain Imaging Behav*. 2020;14. <https://doi.org/10.1007/s11682-018-9995-9>.
- Harnett NG, Stevens JS, van Rooij SJH, Ely TD, Michopoulos V, Hudak L, et al. Multimodal structural neuroimaging markers of risk and recovery from posttrauma anhedonia: a prospective investigation. *Depression Anxiety*. 2021;38:79–88.
- Fani N, Michopoulos V, van Rooij SJH, Clendinen C, Hardy RA, Jovanovic T, et al. Structural connectivity and risk for anhedonia after trauma: A prospective study and replication. *J Psychiatr Res*. 2019;116:34–41.
- Weis CN, Webb EK, Huggins AA, Kallenbach M, Miskovich TA, Fitzgerald JM, et al. Stability of hippocampal subfield volumes after trauma and relationship to development of PTSD symptoms. *Neuroimage* 2021;236. <https://doi.org/10.1016/J.NEUROIMAGE.2021.118076>.
- Li L, Sun G, Liu K, Li M, Li B, Qian SW, et al. White matter changes in posttraumatic stress disorder following mild traumatic brain injury: a prospective longitudinal diffusion tensor imaging study. *Chinese Med J*. 2016;129:1091–9.
- Stout DM, Buchsbaum MS, Spadoni AD, Risbrough VB, Strigo IA, Matthews SC, et al. Multimodal canonical correlation reveals converging neural circuitry across trauma-related disorders of affect and cognition. *Neurobiol Stress*. 2018;9:241–50.
- Harnett NG, Stevens JS, Fani N, van Rooij SJH, Ely TD, Michopoulos V, et al. Acute posttraumatic symptoms are associated with multimodal neuroimaging structural covariance patterns: a possible role for the neural substrates of visual processing in posttraumatic stress disorder. *Biol Psychiatry: Cogn Neurosci Neuroimaging*. 2020. <https://doi.org/10.1016/j.bpsc.2020.07.019>.
- McLean SA, Ressler K, Koenen KC, Neylan T, Germaine L, Jovanovic T, et al. The AURORA study: a longitudinal, multimodal library of brain biology and function after traumatic stress exposure. *Mol Psychiatry*. 2019:1–14.
- Steuber ER, Seligowski AV, Roekner AR, Reda M, Lebois LAM, van Rooij SJH, et al. Thalamic volume and fear extinction interact to predict acute posttraumatic stress severity. *J Psychiatr Res*. 2021;141:325–32.
- Stevens JS, Harnett NG, Lebois LAM, van Rooij JH, Ely TD, Roekner A, et al. Brain-based biotypes of psychiatric vulnerability in the acute aftermath of trauma. *Am J Psychiatry*. 2021;178:1037–49.
- Weathers FW, Litz BT, Keane TM, Palmieri PA, Marx BP, Schnurr PP. The PTSD checklist for DSM-5 (PCL-5). *Natl Cent PTSD*. 2013;5:2002.
- Pilkonis PA, Choi SW, Reise SP, Stover AM, Riley WT, Cella D. Item banks for measuring emotional distress from the patient-reported outcomes measurement information system (PROMIS®): depression, anxiety, and anger. *Assessment*. 2011;18:263–83.
- Weathers FW, Blake DD, Schnurr PP, Kaloupek DG, Marx BP, Keane TM. The life events checklist for DSM-5 (LEC-5) – Extended. National Center for PTSD 2013;5. [http://www.ptsd.va.gov/professional/assessment/te-measures/life\\_events\\_checklist.asp](http://www.ptsd.va.gov/professional/assessment/te-measures/life_events_checklist.asp).
- Weathers FW, Ruscio AM, Keane TM. Psychometric properties of nine scoring rules for the clinician-administered posttraumatic stress disorder scale. *Psychological Assess*. 1999;11:124–33.
- Blake DD, Weathers FW, Nagy LM, Kaloupek DG, Gusman FD, Charney DS, et al. The development of a clinician-administered PTSD scale. *J Trauma Stress*. 1995;8:75–90.
- Gorgolewski K, Burns CD, Madison C, Clark D, Halchenko YO, Waskom ML, et al. Nipype: a flexible, lightweight and extensible neuroimaging data processing framework in Python. *Front Neuroinform*. 2011;5. <https://doi.org/10.3389/fninf.2011.00013>.
- Esteban O, Markiewicz CJ, Blair RW, Moodie CA, Isik AI, Erramuzpe A, et al. fMRIPrep: a robust preprocessing pipeline for functional MRI. *Nat Methods*. 2019;16:111–6.
- Esteban O, Birman D, Schaer M, Koyejo OO, Poldrack RA, Gorgolewski KJ. MRIQC: advancing the automatic prediction of image quality in MRI from unseen sites. *PLoS ONE*. 2017;12:e0184661.
- Douaud G, Smith S, Jenkinson M, Behrens T, Johansen-Berg H, Vickers J, et al. Anatomically related grey and white matter abnormalities in adolescent-onset schizophrenia. *Brain*. 2007;130:2375–86.
- Good CD, Johnsrude IS, Ashburner J, Henson RNA, Friston KJ, Frackowiak RSJ. A voxel-based morphometric study of ageing in 465 normal adult human brains. *Neuroimage*. 2001;14:21–36.
- Smith SM, Jenkinson M, Woolrich MW, Beckmann CF, Behrens TEJ, Johansen-Berg H, et al. Advances in functional and structural MR image analysis and implementation as FSL. *Neuroimage*. 2004. <https://doi.org/10.1016/j.neuroimage.2004.07.051>.

48. Roalf DR, Quarmley M, Elliott MA, Satterthwaite TD, Vandekar SN, Ruparel K, et al. The impact of quality assurance assessment on diffusion tensor imaging outcomes in a large-scale population-based cohort. *Neuroimage*. 2016. <https://doi.org/10.1016/j.neuroimage.2015.10.068>.
49. Andersson JLR, Sotiropoulos SN. An integrated approach to correction for off-resonance effects and subject movement in diffusion MR imaging. *Neuroimage*. 2016;125:1063–78.
50. Wang S, Peterson DJ, Gatenby JC, Li W, Grabowski TJ, Madhyastha TM. Evaluation of field map and nonlinear registration methods for correction of susceptibility artifacts in diffusion MRI. *Front Neuroinform*. 2017;11. <https://doi.org/10.3389/fninf.2017.00017>.
51. Smith SM, Jenkinson M, Johansen-Berg H, Rueckert D, Nichols TE, Mackay CE, et al. Tract-based spatial statistics: voxelwise analysis of multi-subject diffusion data. *Neuroimage*. 2006;31:1487–505.
52. Jahanshad N, Kochunov PV, Sprooten E, Mandl RC, Nichols TE, Almasy L, et al. Multi-site genetic analysis of diffusion images and voxelwise heritability analysis: a pilot project of the ENIGMA-DTI working group. *Neuroimage*. 2013;81:455–69.
53. Pruim RHR, Mennes M, van Rooij D, Llera A, Buitelaar JK, Beckmann CF. ICA-AROMA: a robust ICA-based strategy for removing motion artifacts from fMRI data. *Neuroimage*. 2015;112:267–77.
54. Pruim RHR, Mennes M, Buitelaar JK, Beckmann CF. Evaluation of ICA-AROMA and alternative strategies for motion artifact removal in resting state fMRI. *Neuroimage*. 2015;112:278–87.
55. Satterthwaite TD, Ciric R, Roalf DR, Davatzikos C, Bassett DS, Wolf DH. Motion artifact in studies of functional connectivity: characteristics and mitigation strategies. *Hum Brain Mapp*. 2019;40:2033–51.
56. Beckmann C, Mackay C, Filippini N, Smith S. Group comparison of resting-state fMRI data using multi-subject ICA and dual regression. *Neuroimage*. 2009;47:5148.
57. Nickerson LD, Smith SM, Öngür D, Beckmann CF. Using dual regression to investigate network shape and amplitude in functional connectivity analyses. *Front Neurosci*. 2017;11. <https://doi.org/10.3389/fnins.2017.00115>.
58. Groves AR, Beckmann CF, Smith SM, Woolrich MW. Linked independent component analysis for multimodal data fusion. *Neuroimage*. 2011;54:2198–217.
59. Groves AR, Smith SM, Fjell AM, Tamnes CK, Walhovd KB, Douaud G, et al. Benefits of multi-modal fusion analysis on a large-scale dataset: Life-span patterns of inter-subject variability in cortical morphometry and white matter microstructure. *Neuroimage*. 2012;63:365–80.
60. Itahashi T, Yamada T, Nakamura M, Watanabe H, Yamagata B, Jimbo D, et al. Linked alterations in gray and white matter morphology in adults with high-functioning autism spectrum disorder: a multimodal brain imaging study. *NeuroImage: Clin*. 2015;7:155–69.
61. Li H, Smith SM, Gruber S, Lukas SE, Silveri MM, Hill KP, et al. Denoising scanner effects from multimodal MRI data using linked independent component analysis. *Neuroimage*. 2020;208. <https://doi.org/10.1016/j.neuroimage.2019.116388>.
62. Cox RW. AFNI: software for analysis and visualization of functional magnetic resonance neuroimages. *Computers Biomed Res*. 1996;29:162–73.
63. Clogg CC, Petkova E, Haritou A. Statistical methods for comparing regression coefficients between models. *Am J Sociol*. 1995;100:1261–93.
64. Nir Y, Tononi G. Dreaming and the brain: from phenomenology to neurophysiology. *Trends Cogn Sci*. 2010;14:88–100.
65. Sabatinelli D, Lang PJ, Bradley MM, Costa VD, Keil A. The timing of emotional discrimination in human amygdala and ventral visual cortex. *J Neurosci*. 2009;29:14864.
66. Rudrauf D, David O, Lachaux JP, Kovach CK, Martinerie J, Renault B, et al. Rapid interactions between the ventral visual stream and emotion-related structures rely on a two-pathway architecture. *J Neurosci*. 2008;28:2793.
67. Kark SM, Kensinger EA. Effect of emotional valence on retrieval-related recapitulation of encoding activity in the ventral visual stream. *Neuropsychologia*. 2015;78:221–30.
68. Clewett D, Murty VP. Echoes of emotions past: how neuromodulators determine what we recollect. *eNeuro*. 2019;6. <https://doi.org/10.1523/ENEURO.0108-18.2019>.
69. Weiss DS, Zatzick D, Schoenfeld FB. Sleep disturbances in the Vietnam generation: findings from a nationally representative sample of male Vietnam veterans. *Artic Am J Psychiatry*. 1998. <https://doi.org/10.1176/ajp.155.7.929>.
70. Neylan TC, Marmar CR, Metzler TJ, Weiss DS, Zatzick DF, Delucchi KL, et al. Sleep disturbances in the Vietnam generation: findings from a nationally representative sample of male Vietnam veterans. *Am J Psychiatry*. 1998;155:929–33.
71. Otte C, Lenoci M, Metzler T, Yehuda R, Marmar CR, Neylan TC. Hypothalamic-pituitary-adrenal axis activity and sleep in posttraumatic stress disorder. *Neuropsychopharmacology*. 2005;30:1173–80.
72. Clum GA, Nishith P, Resick PA. Trauma-related sleep disturbance and self-reported physical health symptoms in treatment-seeking female rape victims. *J Nerv Ment Dis*. 2001;189:618.
73. Werner GG, Riemann D, Ehring T. Fear of sleep and trauma-induced insomnia: a review and conceptual model. *Sleep Med Rev*. 2021;55:101383.
74. Levin R, Nielsen TA. Disturbed dreaming, posttraumatic stress disorder, and affect distress: a review and neurocognitive model. 2007. <https://doi.org/10.1037/0033-2909.133.3.482>.
75. Goerke M, Müller NG, Cohrs S. Sleep-dependent memory consolidation and its implications for psychiatry. *J Neural Transm*. 2017;124:163–78.
76. Norman KA, Polyn SM, Detre GJ, Haxby JV. Beyond mind-reading: multi-voxel pattern analysis of fMRI data. *Trends Cogn Sci*. 2006;10:424–30.
77. Connolly AC, Sha L, Swaroop Guntupalli J, Oosterhof N, Halchenko YO, Nastase SA, et al. How the human brain represents perceived dangerousness or “predacity” of animals. *J Neurosci*. 2016;36:5373–84.
78. Yuen EY, Liu W, Karatsoreos IN, Ren Y, Feng J, McEwen BS, et al. Mechanisms for acute stress-induced enhancement of glutamatergic transmission and working memory. *Mol Psychiatry*. 2011;16:156–70.
79. McEwen BS. Protection and damage from acute and chronic stress: allostasis and allostatic overload and relevance to the pathophysiology of psychiatric disorders. *Ann N Y Acad Sci*. 2004;1032:1–7.
80. Yuen EY, Liu W, Karatsoreos IN, Feng J, McEwen BS, Yan Z. Acute stress enhances glutamatergic transmission in prefrontal cortex and facilitates working memory. *Proc Natl Acad Sci USA*. 2009;106:14075–9.
81. Dunsmoor JE, Otto AR, Phelps EA. Stress promotes generalization of older but not recent threat memories. *Proc Natl Acad Sci USA*. 2017;114:201704428.
82. Rabinak CA, Mori S, Lyons M, Milad MR, Phan KL. Acquisition of CS-US contingencies during Pavlovian fear conditioning and extinction in social anxiety disorder and posttraumatic stress disorder. *J Affect Disord*. 2017;207:76–85.
83. Harnett NG, Ference EW, Wood KH, Wheelock MD, Knight AJ, Knight DC. Trauma exposure acutely alters neural function during Pavlovian fear conditioning. *Cortex*. 2018;109:1–13.
84. Gillespie CF, Ressler KJ. Emotional learning and glutamate: translational perspectives. *CNS Spectr*. 2005;10:831.
85. Rosso IM, Crowley DJ, Silveri MM, Rauch SL, Jensen JE. Hippocampus glutamate and N-acetyl aspartate markers of excitotoxic neuronal compromise in post-traumatic stress disorder. *Neuropsychopharmacology*. 2017;42:1698–705.
86. Magarinos AM, Verdugo JMG, McEwen BS. Chronic stress alters synaptic terminal structure in hippocampus. *Proc Natl Acad Sci USA*. 1997;94:14002–8.
87. Harnett NG, Wood KH, Ference EW, Reid MA, Lahti AC, Knight AJ, et al. Glutamate/glutamine concentrations in the dorsal anterior cingulate vary with Post-Traumatic Stress Disorder symptoms. *J Psychiatr Res*. 2017;91:169–76.
88. Bonne O, Brandes D, Gilboa A, Gomori JM, Shenton ME, Pitman RK, et al. Longitudinal MRI study of hippocampal volume in trauma survivors with PTSD. *Am J Psychiatry*. 2001;158:1248–51.
89. Schubert F, Gallinat J, Seifert F, Rinneberg H. Glutamate concentrations in human brain using single voxel proton magnetic resonance spectroscopy at 3 Tesla. *Neuroimage*. 2004;21:1762–71.
90. Yang ZY, Quan H, Peng ZL, Zhong Y, Tan ZJ, Gong QY. Proton magnetic resonance spectroscopy revealed differences in the glutamate plus glutamine/creatine ratio of the anterior cingulate cortex between healthy and pediatric post-traumatic stress disorder patients diagnosed after 2008 Wenchuan earthquake. *Psychiatry Clin Neurosci*. 2015;69:782–90.
91. Logue MW, van Rooij SJH, Dennis EL, Davis SL, Hayes JP, Stevens JS, et al. Smaller hippocampal volume in posttraumatic stress disorder: a multisite ENIGMA-PGC study: subcortical volumetry results from posttraumatic stress disorder consortia. *Biol Psychiatry*. 2018;83:244–53.
92. Nicholson AA, Rabellino D, Densmore M, Frewen PA, Paret C, Kluesch R, et al. The neurobiology of emotion regulation in posttraumatic stress disorder: amygdala downregulation via real-time fMRI neurofeedback. *Hum Brain Mapp*. 2017;38:541–60.
93. Kanstrup M, Singh L, Göransson KE, Widoff J, Taylor RS, Gamble B, et al. Reducing intrusive memories after trauma via a brief cognitive task intervention in the hospital emergency department: an exploratory pilot randomised controlled trial. *Transl Psychiatry*. 2021;11. <https://doi.org/10.1038/s41398-020-01124-6>.
94. Kanstrup M, Kontio E, Geranmayeh A, Olofsdotter Lauri K, Moulds ML, Holmes EA. A single case series using visuospatial task interference to reduce the number of visual intrusive memories of trauma with refugees. *Clin Psychol Psychother*. 2021;28:109–23.

## ACKNOWLEDGEMENTS

We would like to thank the staff at the Institute for Trauma Recovery at UNC, the research assistants for the AURORA study, and all of the participants for their patience, time, and willingness to contribute to this research project. Support for title page creation and format was provided by AuthorArranger, a tool developed at the National Cancer Institute.

## AUTHOR CONTRIBUTIONS

Design and conceptualization of study: RCK, KCK, SM, and KJR. Design and conceptualization of analysis: NGH, KJR, JSS. Data acquisition, recruitment, and logistics: KEF, SEB, SLH, FLB, XA, DZ, TCN, GDC, SDL, LTG, KAB, SLR, CL, PLH, SS, ABS, PIM Jr., JPH, CWJ, BEP, MCK, RAS, LAL, EH, JLP, MJS, AMC, CP, DAP, RMD, NKR, BJON, PS, LDS, DAM, MWM, RHP, JJ, JFS, SHE, and JME. Data processing and statistical analyses: NGH, KEF, LAML, TD, and SVR. Data interpretation: NGH, SVR, TD, LAML, VPM, TJ, KJR, and JSS. Drafting of the manuscript: NGH, SVR, LAML, VPM, TJ, KJR, and JSS. All authors revised the manuscript critically for important intellectual context and agree to be accountable for all aspects of the work in ensuring that questions related to the accuracy or integrity of any part of the work are appropriately investigated and resolved.

## FUNDING

Funding for the study was provided by NIMH K00MH119603, K01MH118467, U01MH110925, the US Army Medical Research and Materiel Command, The One Mind Foundation, and The Mayday Fund. The content is solely responsibility of the authors and does not necessarily represent the official views of any of the funders.

## COMPETING INTERESTS

Dr. Lebois reports unpaid membership on the Scientific Committee for the International Society for the Study of Trauma and Dissociation (ISSTD), grant support from the National Institute of Mental Health, K01 MH118467, and spousal IP payments from Vanderbilt University for technology licensed to Acadia Pharmaceuticals unrelated to the present work. ISSTD and NIMH were not involved in the analysis or preparation of the manuscript. Dr. Neylan has received research support from NIH, VA, and Rainwater Charitable Foundation, and consulting income from Jazz Pharmaceuticals. In the last 3 years, Dr. Clifford has received research funding from the NSF, NIH and LifeBell AI, and unrestricted donations from AliveCor, Amazon Research, the Center for Discovery, the Gordon and Betty Moore Foundation, MathWorks, Microsoft Research, the Gates Foundation, Google, One Mind Foundation, and Samsung Research. Dr. Clifford has financial interest in AliveCor, and receives unrestricted funding from the company. Dr. Clifford also is the CTO of MindChild Medical and CSO of LifeBell AI and has ownership in both companies. These relationships are unconnected to the current work. In the past three years, Dr. Germaine has served on the Scientific Advisory Board of Sage Bionetworks, for which she received a small honorarium. Dr. Rauch reports grants from NIH during the conduct of the study; personal fees from SOBP (Society of Biological Psychiatry) paid role as secretary, other from Oxford University Press royalties, other from APP (American Psychiatric Publishing Inc.) royalties, other from VA (Veterans Administration) per diem for oversight committee, and other from Community Psychiatry/Mindpath Health paid board service, including equity outside the submitted work; other from National Association of Behavioral Healthcare for paid Board service; and Leadership roles on Board or Council for SOBP, ADAA (Anxiety and Depression Association of America), and NNDC (National Network of Depression Centers). Dr. Hendry has received funding from Florida Medical Malpractice Joint Underwriter's Association Dr. Alvin E. Smith Safety of Healthcare Services Grant; Substance Abuse and Mental Health Services Administration (1H79TI083101-01); Overdose Data to Action (OD2A) grant funded by the Centers for Disease Control and Prevention of the U.S. Department of Health and Human Services. Dr. Sheikh has received funding from the Florida Medical Malpractice Joint Underwriter's Association Dr. Alvin E. Smith Safety of Healthcare Services Grant; Allergan Foundation; the NIH/NIA-funded Jacksonville Aging Studies Center (JAX-ASCENT; R33AG05654); and the Substance Abuse and Mental Health Services Administration (1H79TI083101-01); and the Florida

Blue Foundation. Dr. Jones has no competing interests related to this work, though he has been an investigator on studies funded by AstraZeneca, Janssen, Hologic, Inc, and Ophirex. Dr. Joormann receives consulting payments from Janssen Pharmaceuticals. Over the past 3 years, Dr. Pizzagalli has received consulting fees from Boehringer Ingelheim, Compass Pathways, Concert Pharmaceuticals, Engrail Therapeutics, Neumora Therapeutics (former BlackThorn Therapeutics) Neurocrine Biosciences, Neuroscience Software, Otsuka Pharmaceuticals, and Takeda Pharmaceuticals; honoraria from the Psychonomic Society (for editorial work) and Alkermes, and research funding from NIMH, Dana Foundation, Brain and Behavior Research Foundation, and Millennium Pharmaceuticals. In addition, he has received stock options from Compass Pathways, Engrail Therapeutics, Neumora Therapeutics (former BlackThorn Therapeutics) and Neuroscience Software. Dr. Elliott reports support from the National Institutes of Health (NIH) through Grant Numbers R01HD079076 & R03HD094577: Eunice Kennedy Shriver National Institute of Child Health & Human Development; National Center for Medical Rehabilitation Research. He also reports funding from New South Wales Health, Spinal Cord Injury Award (2020–2025) and consulting fees (<\$15,000 per annum) from Orofacial Therapeutics, LLC. In the past 3 years, Dr. Kessler was a consultant for Datastat, Inc., Holmusk, RallyPoint Networks, Inc., and Sage Pharmaceuticals. He has stock options in Mirah, PYM, and Roga Sciences. Dr. Ressler has received consulting income from Alkermes, Jazz Pharma, Bioxel, Bionomics, and Takeda, research support from NIH, Alkermes, Genomind, Alto Neuroscience, and Brainsway, and he has served on advisory boards for Sage, Takeda, Resilience Therapeutics, Janssen and Verily. The remaining authors report no financial interests or potential conflicts of interest.

## ADDITIONAL INFORMATION

**Supplementary information** The online version contains supplementary material available at <https://doi.org/10.1038/s41398-022-02085-8>.

**Correspondence** and requests for materials should be addressed to Nathaniel G. Harnett.

**Reprints and permission information** is available at <http://www.nature.com/reprints>

**Publisher's note** Springer Nature remains neutral with regard to jurisdictional claims in published maps and institutional affiliations.



**Open Access** This article is licensed under a Creative Commons Attribution 4.0 International License, which permits use, sharing, adaptation, distribution and reproduction in any medium or format, as long as you give appropriate credit to the original author(s) and the source, provide a link to the Creative Commons license, and indicate if changes were made. The images or other third party material in this article are included in the article's Creative Commons license, unless indicated otherwise in a credit line to the material. If material is not included in the article's Creative Commons license and your intended use is not permitted by statutory regulation or exceeds the permitted use, you will need to obtain permission directly from the copyright holder. To view a copy of this license, visit <http://creativecommons.org/licenses/by/4.0/>.

© The Author(s) 2022

<sup>1</sup>Division of Depression and Anxiety, McLean Hospital, Belmont, MA, USA. <sup>2</sup>Department of Psychiatry, Harvard Medical School, Boston, MA, USA. <sup>3</sup>Department of Psychiatry and Behavioral Sciences, Emory University School of Medicine, Atlanta, GA, USA. <sup>4</sup>Department of Psychology, Temple University, Philadelphia, PA, USA. <sup>5</sup>Department of Psychiatry and Behavioral Neurosciences, Wayne State University, Detroit, MI, USA. <sup>6</sup>Department of Psychological Sciences, University of Missouri - St. Louis, St. Louis, MO, USA. <sup>7</sup>Department of Emergency Medicine, Washington University School of Medicine, St. Louis, MO, USA. <sup>8</sup>Department of Emergency Medicine & Department of Health Services, Policy, and Practice, The Alpert Medical School of Brown University, Rhode Island Hospital and The Miriam Hospital, Providence, RI, USA. <sup>9</sup>Institute for Trauma Recovery, Department of Anesthesiology, University of North Carolina at Chapel Hill, Chapel Hill, NC, USA. <sup>10</sup>Department of Biostatistics, Gillings School of Global Public Health, University of North Carolina, Chapel Hill, NC, USA. <sup>11</sup>Departments of Psychiatry and Neurology, University of California San Francisco, San Francisco, CA, USA. <sup>12</sup>Department of Biomedical Informatics, Emory University School of Medicine, Atlanta, GA, USA. <sup>13</sup>Department of Biomedical Engineering, Georgia Institute of Technology and Emory University, Atlanta, GA, USA. <sup>14</sup>Institute for Technology in Psychiatry, McLean Hospital, Belmont, MA, USA. <sup>15</sup>The Many Brains Project, Belmont, MA, USA. <sup>16</sup>Department of Psychology and Neuroscience & Department of Sociology, University of North Carolina at Chapel Hill, Chapel Hill, NC, USA. <sup>17</sup>Department of Psychiatry, McLean Hospital, Belmont, MA, USA. <sup>18</sup>Department of Emergency Medicine, University of Massachusetts Chan Medical School, Worcester, MA, USA. <sup>19</sup>Department of Emergency Medicine, Vanderbilt University Medical Center, Nashville, TN, USA. <sup>20</sup>Department of Emergency Medicine, Henry Ford Health System, Detroit, MI, USA. <sup>21</sup>Department of Emergency Medicine, Indiana University School of Medicine, Indianapolis, IN, USA. <sup>22</sup>Department of Emergency Medicine, University of Florida College of Medicine-Jacksonville, Jacksonville, FL, USA. <sup>23</sup>Department of Emergency Medicine, Cooper Medical School of Rowan University, Camden, NJ, USA. <sup>24</sup>Department of Emergency Medicine, Ohio State University College of Medicine, Columbus, OH, USA. <sup>25</sup>Ohio State University College of Nursing, Columbus, OH, USA. <sup>26</sup>Department of Emergency Medicine, University of Alabama School of Medicine, Birmingham, AL, USA. <sup>27</sup>Department of Surgery, Division of Acute Care Surgery, University of Alabama

School of Medicine, Birmingham, AL, USA. <sup>28</sup>Center for Injury Science, University of Alabama at Birmingham, Birmingham, AL, USA. <sup>29</sup>Department of Emergency Medicine, Oakland University William Beaumont School of Medicine, Rochester, MI, USA. <sup>30</sup>Department of Emergency Medicine, Emory University School of Medicine, Atlanta, GA, USA. <sup>31</sup>Department of Surgery, Department of Neurosurgery, University of Pennsylvania, Philadelphia, PA, USA. <sup>32</sup>Perelman School of Medicine, University of Pennsylvania, Philadelphia, PA, USA. <sup>33</sup>Department of Surgery, Division of Traumatology, Surgical Critical Care and Emergency Surgery, University of Pennsylvania, Philadelphia, PA, USA. <sup>34</sup>Einstein Medical Center, Philadelphia, PA, USA. <sup>35</sup>Department of Emergency Medicine, Jefferson University Hospitals, Philadelphia, PA, USA. <sup>36</sup>Department of Emergency Medicine, Wayne State University, Ascension St. John Hospital, Detroit, MI, USA. <sup>37</sup>Department of Emergency Medicine, Massachusetts General Hospital, Boston, MA, USA. <sup>38</sup>Department of Emergency Medicine, Saint Joseph Mercy Hospital, Ypsilanti, MI, USA. <sup>39</sup>Department of Emergency Medicine, University of Massachusetts Medical School-Baystate, Springfield, MA, USA. <sup>40</sup>Department of Emergency Medicine, Wayne State University, Detroit Receiving Hospital, Detroit, MI, USA. <sup>41</sup>Department of Emergency Medicine, McGovern Medical School, University of Texas Health, Houston, TX, USA. <sup>42</sup>Department of Emergency Medicine, Brigham and Women's Hospital, Boston, MA, USA. <sup>43</sup>Department of Emergency Medicine, Harvard Medical School, Boston, MA, USA. <sup>44</sup>National Center for PTSD, Behavioral Science Division, VA Boston Healthcare System, Boston, MA, USA. <sup>45</sup>Department of Psychiatry, Boston University School of Medicine, Boston, MA, USA. <sup>46</sup>National Center for PTSD, Clinical Neurosciences Division, VA Connecticut Healthcare System, West Haven, CT, USA. <sup>47</sup>Department of Psychiatry, Yale School of Medicine, New Haven, CT, USA. <sup>48</sup>Department of Psychology, Yale University, New Haven, CT, USA. <sup>49</sup>Department of Psychological & Brain Sciences, Washington University in St. Louis, St. Louis, MO, USA. <sup>50</sup>Division of Biosciences, Ohio State University College of Dentistry, Columbus, OH, USA. <sup>51</sup>Institute for Behavioral Medicine Research, OSU Wexner Medical Center, Columbus, OH, USA. <sup>52</sup>Department of Anesthesiology, University of Michigan Medical School, Ann Arbor, MI, USA. <sup>53</sup>Department of Internal Medicine-Rheumatology, University of Michigan Medical School, Ann Arbor, MI, USA. <sup>54</sup>Kolling Institute, University of Sydney, St Leonards, New South Wales, Australia. <sup>55</sup>Faculty of Medicine and Health, University of Sydney, Northern Sydney Local Health District, New South Wales, Australia. <sup>56</sup>Physical Therapy & Human Movement Sciences, Feinberg School of Medicine, Northwestern University, Chicago, IL, USA. <sup>57</sup>Department of Health Care Policy, Harvard Medical School, Boston, MA, USA. <sup>58</sup>Department of Epidemiology, Harvard T.H. Chan School of Public Health, Harvard University, Boston, MA, USA. <sup>59</sup>Department of Emergency Medicine, University of North Carolina at Chapel Hill, Chapel Hill, NC, USA. <sup>60</sup>Institute for Trauma Recovery, Department of Psychiatry, University of North Carolina at Chapel Hill, Chapel Hill, NC, USA. <sup>61</sup>McLean Imaging Center, McLean Hospital, Belmont, MA, USA. <sup>62</sup>email: nharnett@mclean.harvard.edu